Optics Letters

Fiber-format dual-comb coherent Raman spectrometer

Nicola Coluccelli,[1,2,*] Christopher R. Howle,[3] Kenneth McEwan,[3] Yuchen Wang,[1] Toney Teddy Fernandez,[1] Alessio Gambetta,[1] Paolo Laporta,[1,2] and Gianluca Galzerano[2]

[1]Dipartimento di Fisica—Politecnico di Milano, Piazza Leonardo da Vinci 32, 20133 Milano, Italy
[2]Istituto di Fotonica e Nanotecnologie—CNR, Piazza Leonardo da Vinci 32, 20133 Milano, Italy
[3]Defence Science and Technology Laboratory, Porton Down, Salisbury SP4 0JQ, UK
*Corresponding author: nicola.coluccelli@polimi.it

Received 5 September 2017; revised 16 October 2017; accepted 16 October 2017; posted 16 October 2017 (Doc. ID 306477); published 9 November 2017

We demonstrate a fiber-format system for dual-comb coherent anti-Stokes Raman scattering spectroscopy. The system is based on two ytterbium fiber (Yb) femtosecond lasers at repetition frequencies of 94 MHz, a Yb amplifier, and a photonic crystal fiber for spectral broadening and generation of pulses with a central wavelength of 1040 nm and durations in the sub-20-fs regime. We observed Raman spectra of acetonitrile and ethyl acetate with spectral coverage from 100 to 1300 cm^{-1}, resolution of 8 cm^{-1}, and a signal-to-noise ratio of around 100, when averaging over 10 acquisitions. The design is suitable for implementing portable dual-comb coherent Raman spectrometers.

OCIS codes: (140.3510) Lasers, fiber; (320.0320) Ultrafast optics; (300.6230) Spectroscopy, coherent anti-Stokes Raman scattering.

https://doi.org/10.1364/OL.42.004683

Over the past decade, coherent anti-Stokes Raman scattering (CARS) has been used increasingly as a noninvasive spectroscopic tool in biophysics, biology, and material sciences, offering 3D imaging capability and chemical specificity without the need of fluorescence labeling [1]. Several techniques have been explored, including coherent control CARS [2], time-resolved CARS [3], Fourier-transform CARS [4–6], interferometric CARS [7], and frequency-modulation CARS (FM-CARS) [8]. Besides these, a dual-comb CARS technique has been proposed recently [9,10] featuring broadband operation and short measurement time on the μs-ms time scale, and resolution limited by the intrinsic width of the molecular resonance. Dual-comb CARS is based on using two combs at slightly different repetition frequencies to excite and probe a molecular sample by pairs of femtosecond pulses in a typical two-photon Raman process. The pulses of the first comb excite molecular vibrations decaying within times proportional to the corresponding coherence times (10–100 ps). The blue-shifted CARS beam originating at the sample is then probed by the second comb pulses at linearly increasing time delay, and the resulting interferogram is Fourier-transformed to retrieve the Raman spectrum of the molecules [9].

As for the comb sources, Ti:sapphire lasers have been adopted until now for dual-comb CARS experiments, allowing for observation of high-quality Raman spectra in the range from 200 to 1400 cm^{-1}, with signal-to-noise ratio (SNR) as high as 10^3 and resolution down to 4 cm^{-1} [9,10]. As the spectral span of dual-comb CARS is basically limited by the bandwidth of the comb source, Ti:sapphire lasers represent a straightforward solution for broadband excitation and probing of the molecular sample; however, these sources are bulky and require maintenance (daily alignment) by skilled personnel within a laboratory environment. For practical applications, an approach based on fiber laser combs is favored. In this Letter, we present a fiber-format dual-comb CARS system based on ytterbium fiber (Yb) and photonic crystal fiber (PCF) technology. The proposed design features two low-power Yb-fiber femtosecond lasers operating at repetition frequency of 94 MHz, a Yb-fiber amplifier, and a positive-dispersion PCF for smooth spectral broadening allowing for the generation of coherent pulses at 1040 nm compressible to sub-20-fs durations. The Raman spectra of acetonitrile and ethyl-acetate liquid samples have been observed in the range from 100 to 1300 cm^{-1} with SNR of ~25 and acquisition times of 20 μs on a single acquisition. The SNR is improved to 100 (acquisition time of 0.5 s) when averaging over 10 acquisitions.

The experimental layout adopted during dual-comb CARS experiments is presented in Fig. 1. The core of the system comprises two homemade Yb-fiber femtosecond oscillators operating at repetition frequencies of $f_{r1} = 94$ MHz and $f_{r2} = f_{r1} + \Delta f$, with Δf typically set in the range 0 to 100 Hz. The oscillators are based on typical architecture of femtosecond fiber lasers mode-locked by nonlinear polarization rotation [11]; they share the same cavity architecture and are pumped by two single-mode pump diodes operating at 976 nm with an output power of 300 mW. The pump beam is injected inside the laser cavities through standard wavelength division multiplexers (WDMs). The gain fibers are highly doped Yb fibers (Yb1200-4/125, core diameter 4 μm, NA 0.2) with a length of 70 cm. The group-velocity dispersion (GVD) of

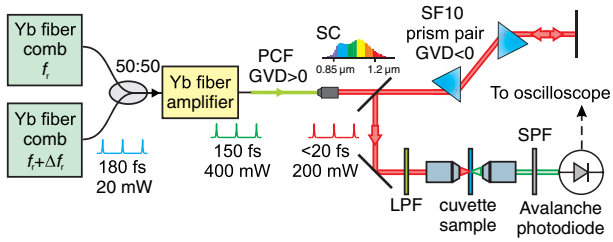

Fig. 1. Layout of the fiber-format dual-comb CARS spectrometer. PCF, photonic crystal fiber; SC, supercontinuum; LPF, long-pass filter; SPF, short-pass filter.

the gain fiber is 23 fs^2/mm. On one end, each gain fiber is spliced to a HI1060 fiber (40 cm, GVD of 24 fs^2/mm) terminated by a collimator whereas the other end is spliced to a WDM through another HI1060 fiber (40 cm). The output of the WDM is a HI1060 fiber (41 cm) terminated by a collimator. The laser cavities also have a free-space section (36 cm long) consisting of two quarter-waveplates and a half-waveplate for control of the mode-locking regime, a polarizing beam splitter cube for output coupling, a grating compressor, and an isolator. The grating compressor comprises two transmission gratings (1000 lines/mm) providing compensation of the GVD inside the laser cavity by fine tuning of the grating distance. By setting the grating distance to 7 mm (estimated GVD of −1330 fs^2/mm), a pure soliton mode-locking regime is induced by nonlinear polarization rotation in the fibers. Unidirectional operation is guaranteed by intracavity isolators. Additional grating compressors (1000 lines/mm) are placed at the output of the laser cavities for proper prechirping of the pulses before amplification. Specifically, the distance between the gratings of the external compressor is set to 8 mm, corresponding to a group delay dispersion (GDD) of −10640 fs^2. Figure 2(a) shows the typical spectrum of an oscillator with full width at half-maximum (FWHM) band of 7 nm at an output power level of 25 mW. The repetition frequencies are adjusted by piezoelectric transducers acting on the laser cavity length. Two low-bandwidth control loops phase-lock the repetition frequencies to external reference signals generated by a frequency synthesizer.

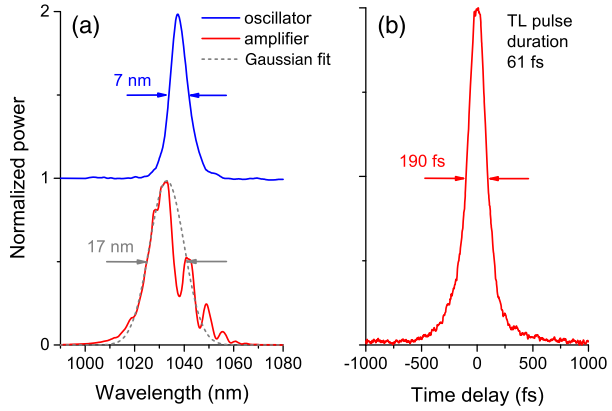

Fig. 2. (a) Output spectra of Yb-fiber oscillator (blue line) and amplifier (red line); the gray dotted line represents the Gaussian fit to the amplifier output spectrum. (b) Autocorrelation trace of pulses at the output of the Yb-fiber amplifier.

As solitonic mode-locked Yb-fiber oscillators cannot be operated at high power due to the onset of multiple pulsing, a femtosecond Yb-fiber amplifier has been implemented. Before seeding the amplifier, the beams from the two oscillators are passed through isolators, multiplexed through a 50:50 combiner, and then coupled into a WDM. At this point, both beams are propagated through the same fiber; hence, the spatial overlap is self-guaranteed and does not need optimization to permit generation of the dual-comb CARS signal as in free-space systems based on Ti:sapphire oscillators. Taking into account the additional optics and fibers, the power coupled into the WDM is around 7 mW (each oscillator).

The amplifier pump diode operates at 976 nm with a maximum optical power of 1 W. The gain fiber is a highly doped Yb fiber (Yb1200-6/125-DC, core diameter 6 μm, NA 0.12) with a length of 22 cm. A HI1060 fiber (32 cm) guides the pulses to the amplifier input. It is worth noting that the gain fiber adopted in the amplifier is different from the oscillator; specifically, it has a larger core diameter of 6 μm that is beneficial to reduce nonlinear distortion of the seed pulses when propagating through the amplifier. To the same purpose, the negative prechirp given to the solitons at the output of the oscillators has to be properly tuned by adjusting the distance between the gratings in the extra-cavity compressors for the best tradeoff. More specifically, on the one hand the prechirp has to be sufficiently large to avoid excess distortions of the soliton spectral shape, detrimental for subsequent generation of broadband compressible pulses by the PCF [12,13]; on the other hand, the prechirp should be not too large because this would result in only modest spectral broadening within the following PCF, reducing the spectral coverage of the dual-comb CARS spectra. Figure 2(a) shows the spectrum of the amplified soliton at the output of the Yb-fiber amplifier, with a power of 450 mW, obtained when both oscillators are injected into the amplifier; a modest amount of nonlinear broadening increases the band of the solitons to around 17 nm, as estimated by the Gaussian fit. The duration of the pulses at the output of the amplifier has been measured using an autocorrelator based on noncollinear second-harmonic generation. The result is shown in Fig. 2(b), where the FWHM duration of the autocorrelation trace is 190 fs. However, the corresponding transform-limited (TL) duration has been calculated to be 61 fs, meaning that a residual positive chirp is characterizing the pulses at this point of the system; this has been also confirmed by insertion of negative GDD by multiple reflections on chirped mirrors.

To reach sufficient spectral coverage in dual-comb CARS measurements, the amplified pulses have been spectrally broadened using a positive dispersion PCF (NKT Photonics, NL-1050-NEG-1) with a length of 75 mm that has been fusion spliced to the output end of the amplifier fiber. Optimization of the splicing parameters yielded very high stability of the joint and splice losses of 30%. Figure 3(a) shows the supercontinuum radiation at the output of the PCF when both oscillators are seeding the amplifier, with a power content of about 300 mW. The bandwidth spanned by the continuum is slightly reduced when both lasers are injected into the amplifier due to gain saturation, as the pump power available is shared by both lasers; nonetheless, a notable bandwidth of 150 nm is obtained when both lasers seed the amplifier. Additionally, a residual pump power of nearly 25 mW is present in the supercontinuum.

The coherence of the obtained supercontinuum and potential for pulse compression has been tested. The GVD of the PCF used here is 8 fs^2/mm at 1040 nm, a very low dispersion compared to standard fibers; taking into account the fiber length of 75 mm, this corresponds to a total GDD contribution of 585 fs^2. A prism compressor based on SF10 prisms has been used for pulse compression. Figure 3(b) shows the autocorrelation trace of the compressed pulses at the output of the PCF, with a FWHM of 26 fs, as measured when both oscillators seed the amplifier. Additionally, the TL pulses and corresponding autocorrelation [shown also in Fig. 3(b)] have been calculated starting from the measured supercontinuum spectrum. The experimental and calculated TL autocorrelations closely match, apart from a small pedestal in the experimental trace ascribed to some amount of third-order dispersion that is not fully compensated by the SF10 prism compressor. However, as the TL pulse has an estimated FWHM duration of 17 fs, it can be inferred that the experimental pulse has a duration in the sub-20-fs regime. The average power of the pulse train at the output of the prism compressor is around 200 mW (both oscillators on), sufficiently high for dual-comb CARS detection.

A preliminary demonstration of the potential for dual-comb CARS detection has been obtained with a sample of pure acetonitrile (CH_3 – CN, CAS number 75-05-8) in liquid phase. In particular, the pulse trains at the output of the PCF, with repetition frequencies set to $f_{r1} \cong 94$ MHz and $f_{r2} = f_{r1} + \Delta f$, with Δf in the range of 2–20 Hz, are first collimated by a high-numerical aperture lens. They are then passed through an optical long-pass filter (LPF, cutoff around 940 nm, 10638 cm^{-1}) and finally focused onto the liquid sample within a quartz cuvette (3-mm length) with a focusing lens of 8-mm focal length. The pulse energy at the sample is around 1 nJ for each comb. The generated anti-Stokes beam and the residual comb beams are collimated using another lens of 8-mm focal length. Afterward, the beams pass through an optical short-pass filter (SPF, cutoff wavelength of 915 nm, 10929 cm^{-1}) for optimizing the CARS spectrum and filtering out the light from the PCF. Figure 4 shows the anti-Stokes Raman spectrum generated by the acetonitrile sample when the beams from both oscillators are simultaneously focused onto the sample. The CARS spectrum extends from 810 (12346 cm^{-1}) to 910 nm (10989 cm^{-1}), corresponding to a Raman frequency span of ~1350 cm^{-1}. If one oscillator is blocked, the amplifier gain is all exploited by the unblocked (remaining) beam, resulting in a broader supercontinuum and hence a broader Raman spectrum extending down to 790 nm, as experimentally verified.

The anti-Stokes interferogram resulting from beating of the combs from the two oscillators is detected by a 50-MHz-bandwidth silicon avalanche photodiode. The electronic signal from the PD is low-pass filtered (cutoff at 15 MHz) and amplified with a low-noise 20-dB gain voltage amplifier. The signal is then digitized using a 12-bit oscilloscope with a sampling rate of 250 MS/s. The Fourier transform of the interferogram reveals the CARS spectrum of the sample; however, a proper time window (rectangular shape) has to be applied to the interferogram to select only the relevant signal and reject nonresonant contribution (CARS background and residual combs). Additionally, it is worth noting that gain saturation in the amplifier when the two comb pulses are overlapping results in some dual-comb interferogram distortion, which can be seen in the tail of the nonresonant background. This distortion can be windowed out by delaying the Fourier transformation; however, it reduces the relevant part of the interferogram that contains the CARS ringing signals and, hence, the SNR of the spectral features. A system configuration with two Yb-fiber amplifiers separately seeded by each comb should be beneficial to avoid this distortion. Typical dual-comb CARS spectra of pure acetonitrile measured under different experimental conditions are shown in Fig. 5. The Raman range covered by the Yb-fiber

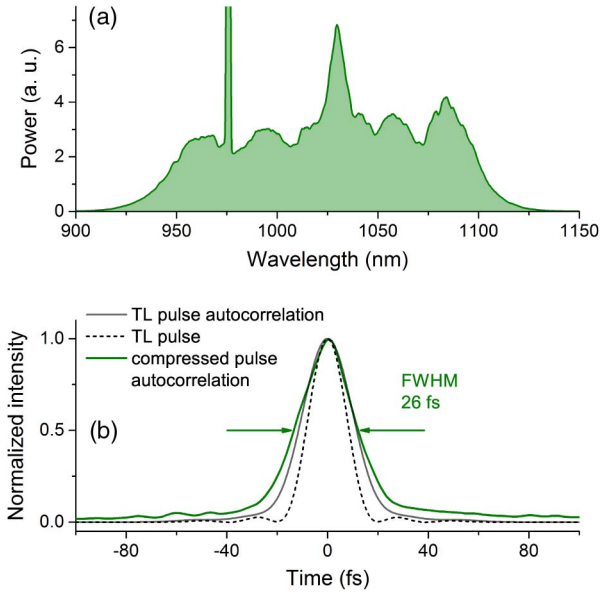

Fig. 3. (a) Spectrum of the supercontinuum radiation generated by the PCF fiber; the peak at 980 nm is due to residual pump power. (b) Autocorrelation trace of compressed pulses as measured after the SF10 prism pair (green line) and of transform-limited pulses (gray line). The transform-limited pulses of 17-fs duration are also represented (dotted line).

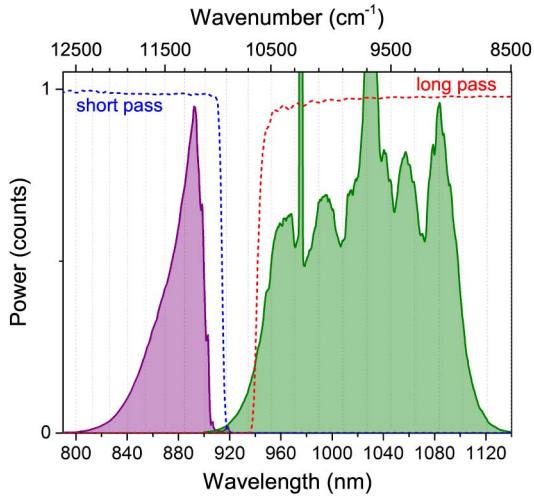

Fig. 4. Spectrum of radiation incident onto the sample prior to long-pass filtering (green line) and spectrum of a typical dual-comb CARS signal generated by the sample after short-pass filtering (purple line). The transmittance of the short- and long-pass filters adopted in the detection unit are also plotted (blue- and red-dotted line, respectively). Spectra are not to scale.

dual-comb CARS spectrometer extends from 100 to 1300 cm^{-1}, where two strong resonances of acetonitrile at 382 and 921 cm^{-1} are detected. The reduced amplitude of the peak at 382 cm^{-1} with respect to the reference spectrum (also shown in Fig. 5) is due to the filtering action of the LPF, allowing only for a reduced number of anti-Stokes comb lines to reach the PD and contribute to the low-frequency tail of the Raman spectrum. Similarly, the sensitivity at high Raman frequency close to 1300 cm^{-1} is limited by the reduced number of lines in the comb tails allowing for excitation of high-frequency molecule vibrations. In particular, when setting Δf to 20 Hz, the SNR of the most intense peak at 921 cm^{-1} (C-C stretching mode) reaches a value of 25 on a single interferogram with observation time of 20 μs. The resolution of the measurement is 8 cm^{-1}, slightly higher than the 5 – cm^{-1} FWHM of the Raman resonance retrieved from the reference spectra of acetonitrile. This is ascribed to the additional phase noise introduced by the PCF during spectral broadening of the amplified pulses. The effect is even more pronounced when setting Δf to 2 Hz: in this case, even though the SNR increases to 55, thanks to the longer duration of the exponential decay of the Raman vibrations in the interferogram, the linewidth of the combs is apparently increased, and the resulting resolution in the dual-comb CARS spectrum is limited to 42 cm^{-1}. Notably, the SNR can be improved to 100, while keeping the resolution at 8 cm^{-1} when averaging over 10 interferograms. In this case, to avoid the degradation of resolution due to the comb frequency noise, a software routine has been embedded into the oscilloscope to calculate the average frequency of the main peak over the subsequent spectra and rescale correspondingly the frequency axis to align the peaks [10]. As a further demonstration of potential for dual-comb CARS applications, the spectrum of ethyl acetate ($CH_3 - COO - CH_2 - CH_3$, CAS number 141-78-6) has been measured with Δf set to 15 Hz, and the result is reported in Fig. 6 together with the reference spectrum. The three main resonances of ethyl acetate at 381, 638, and 851 cm^{-1} are clearly detected, and according to the lower Δf adopted in this measurement, the SNR on the main peak at 638 cm^{-1} reaches a value of 36. Notably, the weaker resonances at 1005 and

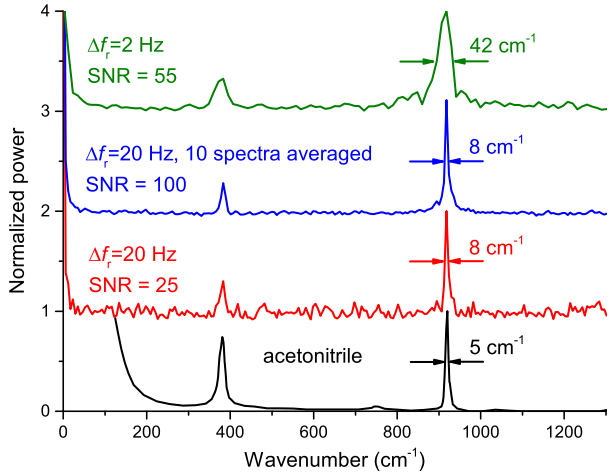

Fig. 5. Dual-comb CARS spectra calculated by Fourier-transform of the interferograms under different measuring conditions (red, blue, and green lines), and reference Raman spectrum of pure acetonitrile [14].

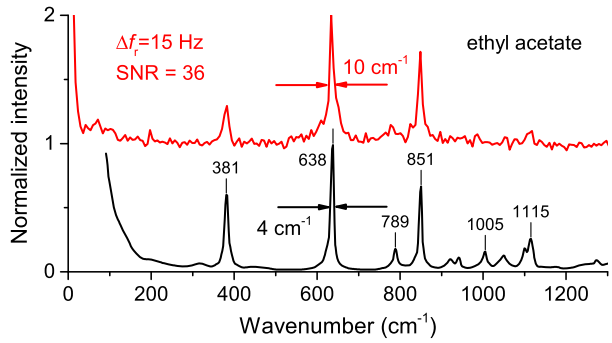

Fig. 6. Dual-comb CARS spectrum of ethyl acetate (red line), as calculated by Fourier transform of a single-windowed interferogram (30 μs observation time) and reference Raman spectrum of pure ethyl acetate [15].

1115 cm^{-1} can be seen above the noise floor; however, they are characterized by a low SNR. The spectrum has been measured by Fourier transform of a single interferogram with a time window (no apodization) of 30 μs.

In conclusion, a proof-of-concept of a fiber-format spectrometer for dual-comb CARS detection has been demonstrated with liquid samples of acetonitrile and ethyl acetate observed in the Raman range from 100 to 1300 cm^{-1}. A single interferogram acquisition allowed for reaching a SNR of 36 with an observation time of 30 μs; the SNR can be improved to 100 when averaging over 10 interferograms, with an acquisition time of 0.5 s. Being based on fiber technology, the system is very promising for practical and "on field" applications of the dual-comb CARS technique to any kind of condensed phase chemicals.

Funding. Defence and Security Accelerator, part of the UK Ministry of Defence (DSTLX-1000107010).

REFERENCES

1. C. L. Evans and X. S. Xie, Annu. Rev. Anal. Chem. **1**, 883 (2008).
2. D. Oron, N. Dudovich, and Y. Silberberg, Phys. Rev. Lett. **90**, 213902 (2003).
3. R. Selm, M. Winterhalder, A. Zumbusch, G. Krauss, T. Hanke, A. Sell, and A. Leitenstorfer, Opt. Lett. **35**, 3282 (2010).
4. M. Cui, M. Joffre, J. Skodack, and J. P. Ogilvie, Opt. Express **14**, 8448 (2006).
5. M. Tamamitsu, Y. Sakaki, T. Nakamura, G. K. Podagatlapalli, T. Ideguchi, and K. Goda, Vib. Spectrosc. **91**, 163 (2017).
6. K. Hashimoto, M. Takahashi, T. Ideguchi, and K. Goda, Sci. Rep. **6**, 21036 (2016).
7. D. L. Marks, C. Vinegoni, J. S. Bredfeldt, and S. A. Bopparta, Appl. Phys. Lett. **85**, 5787 (2004).
8. F. Ganikhanov, C. L. Evans, B. G. Saar, and X. S. Xie, Opt. Lett. **31**, 1872 (2006).
9. T. Ideguchi, S. Holzner, B. Bernhardt, G. Guelachvili, N. Picqué, and T. W. Hansch, Nature **502**, 355 (2013).
10. K. J. Mohler, B. J. Bohn, M. Yan, G. Melen, T. W. Hansch, and N. Picqué, Opt. Lett. **42**, 318 (2017).
11. X. Li, M. A. R. Reber, C. Corder, Y. Chen, P. Zhao, and T. K. Allison, Rev. Sci. Instrum. **87**, 093114 (2016).
12. S. R. Domingue and R. A. Bartels, Opt. Express **21**, 13305 (2013).
13. H. Tu, Y. Liu, J. Laegsgaard, U. Sharma, M. Siegel, D. Kopf, and S. A. Boppart, Opt. Express **18**, 27872 (2010).
14. http://www.chemicalbook.com/SpectrumEN_75-05-8_Raman.htm.
15. http://www.chemicalbook.com/SpectrumEN_141-78-6_Raman.htm.